PNAS RESEARCH ARTICLE | PLANT BIOLOGY

The ER–PM interaction is essential for cytokinesis and recruits the actin cytoskeleton through the SCAR/WAVE complex

Zhijing Xu[a,b], Jingze Zang[a,b], Xintong Zhang[a,b], Qiwei Zheng[a,b], Yifan Li[a,b], Nadine Field[c], Jindriska Fiserova[d], Bing Hua[e], Xiaolu Qu[a,b], Verena Kriechbaumer[c], Michael J. Deeks[f], Patrick J. Hussey[d], and Pengwei Wang[a,b,1]

Affiliations are included on p. 10.

Edited by Bo Liu, University of California, Davis, CA; received August 21, 2024; accepted December 27, 2024 by Editorial Board Member Rebecca Heald

Plant cytokinesis requires coordination between the actin cytoskeleton, microtubules, and membranes to guide division plane formation and cell plate expansion; how these regulatory factors are coordinated remains unknown. The actin cytoskeleton assembly is controlled by several actin nucleation factors, such as the SCAR/WAVE complex, which regulates actin nucleation and branching through the activation of the ARP2/3 complex. The activity of these actin regulatory proteins is likely influenced by interactions with specific membranes; however, the molecular basis and the biological relevance of SCAR–membrane interactions are also unclear. In this study, we demonstrate that the ER–PM tethering protein VAP27-1 directly interacts with SCAR2 at the ER membrane and that they colocalize to guide cell plate orientation during cell division. In the root meristem, both VAP27-1 and SCAR2 exhibit polarized localization at the cell plates, where the interaction between ER and PM is abundant. VAP27-1 recruits SCAR2 to the cell division plane, where there is a high concentration of actin filaments. In the *vap27-1346* mutant, the densities of cortical ER, SCAR2, and consequently actin filaments are significantly reduced at the cell division plane, affecting cell plate orientation, cell division, and root development. A similar phenomenon is also observed in the *scar1234* mutant, suggesting that VAP27 and SCAR proteins regulate cell division through a similar pathway. In conclusion, our data reveal a plant-specific function of VAP27-regulated ER–PM interaction and advance our understanding of plant ER–PM contact site and its role in cell division.

ER–PM contact sites | actin cytoskeleton | endoplasmic reticulum | SCAR/WAVE complex | cytokinesis

Significance

Plant cytokinesis requires the contribution of the cytoskeleton and membrane systems, but how actin interacts with these membrane structures is poorly understood. Here, we demonstrate that the VAP27-regulated ER–PM interaction is critical for recruiting the ER network to the cell division plane together with SCAR, which is part of a complex known to activate actin polymerization. These findings reveal a plant-specific function of the ER–PM contact sites and advance our understanding of cytoskeleton–membrane interactions and their role in cell division.

The actin cytoskeleton is a highly dynamic structure that regulates many biological activities in plants, such as organelle movement, cell morphogenesis, and polarized cell growth. It assembles and disassembles rapidly in response to different environmental and developmental cues, and this rapid remodeling is regulated by specific actin-binding proteins. The ARP2/3 complex is one of the best-known regulators that control actin nucleation, assembly, and branching (1), maintaining cytoskeletal homeostasis and normal plant development (2). The activity of the ARP2/3 complex is controlled by various nucleation-promoting factors, such as the SCAR/WAVE complex that is composed of five different subunits (SCAR, NAP1, PIR121, ABI1, and BRICK1/HSPC300), with the SCAR subunit playing central roles. There are four SCAR homologs identified in the *Arabidopsis* genome; it contains a C-terminal VCA domain that binds to the ARP2/3 complex and an N-terminal SH domain that interacts with other subunits required for actin nucleation (3–5). The sequence similarity of plant SCAR is very low compared to its animal homologs, suggesting that it might be involved in unique activities in plants. For example, SCAR2 exhibits polarized localization in epidermal cells and root hairs, regulating root hair development and asymmetric cell division (6–8). Several members of the ARP2/3 and SCAR/WAVE complexes have been reported to interact with membrane structures to participate in different activities (9, 10), such as mediating light signal transduction and autophagy (11–13). In plants, these proteins were likely enriched in the ER network, but whether such ER association is essential for the activity of SCAR/WAVE is not known (9).

The endoplasmic reticulum (ER) is a complex membrane network whose dynamics are mainly driven by the actin cytoskeleton in plants (14–19). Cortical ER is also closely associated with the plasma membrane (PM) through several ER–PM tethering proteins at the membrane contact sites (MCS) (20, 21). VAP27 is the plant homolog of the yeast Scs2 protein, which localizes at ER–PM contact sites (EPCS) and interacts with actin filaments and microtubules, suggesting that a close interaction among ER, PM, and the

Author contributions: Z.X., J.Z., P.J.H. and P.W. designed research; Z.X., X.Z., Q.Z., Y.L., N.F., J.F., M.J.D and B.H. performed research; X.Q. contributed new reagents/analytic tools; Z.X., V.K., M.J.D., P.J.H. and P.W. analyzed data; and Z.X., P.J.H and P.W. wrote the paper.

The authors declare no competing interest.

This article is a PNAS Direct Submission. B.L. is a guest editor invited by the Editorial Board.

[1]To whom correspondence may be addressed. Email: wangpengwei@mail.hzau.edu.cn.

This article contains supporting information online at https://www.pnas.org/lookup/suppl/doi:10.1073/pnas.2416927122/-/DCSupplemental.

Published February 6, 2025.

cytoskeleton exists in plants (18, 22). Further studies revealed that plant-specific cytoskeletal binding proteins are associated with the EPCS, such as the NET (NETWORKED) and IQD (IQ67 DOMAIN proteins) family, which regulate the organization of actin and microtubules, respectively (23–25). It is well known in all eukaryotic cells that the cytoskeleton contributes to membrane dynamics and organization. However, recent studies in plants suggested that membrane structure can also influence cytoskeletal function. When the ER morphology is altered by overexpressing some ER shaping proteins, the distribution and density of actin filaments also changes accordingly (14), indicating some cytoskeletal regulators may associate with the ER surface through an unknown mechanism.

Cytokinesis in plants requires the formation of the cell plate at the division plane, which contains highly ordered microtubule bundles and actin filaments (26–28). In most previous studies, the importance of microtubules in cell division plane establishment has been well reported (29–31), and the roles of actin have only started to be elucidated. It has been shown that myosin motor proteins play a crucial role in cell division, particularly in cell division plane orientation. In the myosin XI-K triple knockout mutant, an increase in the number of oblique cell walls was observed (32). In *Physcomitrium patens,* myosin VIII and XI play a role in guiding cell plate expansion, and their function is dependent on actin nucleating protein *Pp*Formin 2 and the actin cytoskeleton (33, 34).

Some transmission electron microscopy (TEM) and laser confocal microscopy (LCM) studies also revealed that the cisternae ER branch forms narrow ER tubes across the cell plate (35–38). The ER membrane is accumulated at the edge of the cell plate, facilitating the expansion and fusion with the parent cell (39). In *Physcomitrium patens*, interrupting ER function by knocking out some ER localized protein (e.g., SABRE) leads to abnormal cell plate development (40), suggesting that the ER is an essential regulator of plant cytokinesis. Still, its mechanisms of action are largely unknown. In fission yeast, the ER–PM contact sites and Scs2 protein restrict the assembly of the actin contractile ring to determine the division sites and define actomyosin kinetics (41). In plants, the disruption of actin also delays cell plate expansion and inhibits the ER accumulation in the cell plate during cytokinesis (42). Therefore, there must be a precisely coordinated mechanism that regulates microtubules, actin, and ER networks during cell plate formation. On the other hand, as the cell plate and cell division plane are enriched in cytoskeletal components, PM, and the ER network, it might be considered a specialized region that consists of intensive ER–PM interactions.

In this study, we demonstrate a direct interaction between the ER–PM tethering protein, VAP27 and SCAR, a member of the SCAR/WAVE complex, and that they exhibit a polarized localization at the newly formed cell plates. The recruitment of SCAR, actin filaments, and ER membrane to the cell plate is inhibited in the absence of VAP27. In *vap27-1346* and *scar1234* mutants root development, meristem cell number and cell plate orientation are significantly affected, suggesting that VAP27 underpins SCAR-regulated actin assembly during cell division and cell plate expansion. Taken together, our findings provide solid evidence that the ER and ER–PM interactions are essential for cytokinesis and are reliant on the interaction between VAP27 and SCAR proteins.

Results

SCAR2 was Identified to Interact with VAP27 from a Yeast Two-Hybrid Screen. The SCAR/WAVE and ARP2/3 complexes are essential for actin assembly and dynamics, and this regulatory module is conserved in most eukaryotic cells. In animals, these actin nucleators are required for cell movement and embryogenesis, which is essential for life (43). However, mutating proteins of the SCAR/WAVE complex in plants does not cause lethality, allowing the underlying effects of these mutations to be studied (10, 44). To further understand the regulatory mechanism of the SCAR/WAVE complex in plants, we performed a yeast two-hybrid screen using SCAR2 (a key component of the complex). We identified a possible interaction with VAP27 (*SI Appendix*, Table S1 and Fig. S1), a family of conserved integral ER membrane proteins that are also known as VAMP-associated proteins (VAPs) and Scs2 in animals and yeast, respectively (22). Ten VAP homologs have been identified in *Arabidopsis*, and most proteins of this family are localized to various ER–MCS (45), with the ER–PM contact sites being the most well studied. First, we constructed the pVAP27-1:VAP27-1-mCherry (hereafter VAP27-mCh) and p35S:GFP-SCAR2 (hereafter GFP-SCAR2) vectors and transiently transformed them into *N. benthamiana* leaf epidermal cells. When both proteins are coexpressed, VAP27-mCh recruits GFP-SCAR2 onto the ER membrane; in contrast, the SCAR2 is solely cytoplasmic when it expressed alone (Fig. 1*A*). In agreement with this observation, the bimolecular fluorescence complementation (BiFC) assay also suggested that most of the nYFP–SCAR2 and cYFP–VAP27-1 interacting signals were ER-associated (Fig. 1*B*). This interaction was further confirmed in vitro using a GST pull-down assay, the full-length MBP-VAP27-1 protein stays associated with a GST-SCAR2 truncational mutant (a.a. 1 to 432, Fig. 1*C*). In *Arabidopsis*, the VAP27 and SCAR proteins have multiple homologs (3, 4, 45), so one-on-one yeast two-hybrid tests were performed between combinations of different VAP27 and SCAR isoforms. The results indicate that SCAR1, 2, and 3 have the capacity to interact with multiple VAP27 proteins (Fig. 1*D*), suggesting the interaction is likely conserved among different members of the two families. Here, we concentrated on the interaction between VAP27-1 and SCAR2 for most cell biology and microscopical studies to avoid repetition.

Next, we obtained transgenic *Arabidopsis* lines stably expressing VAP27-1-GFP (hereafter VAP27-GFP) and SCAR2-mCherry (hereafter SCAR2-mCh) driven by its native promoters (6, 45). Both proteins are globally expressed with the strongest signals at the root tips. Subsequent observation revealed that VAP27-1 is localized at the cell peripheral and the ER membrane, while SCAR2 is mainly at the PM in root cells (Fig. 1 *E* and *F*). Interestingly, both proteins exhibit polarized localization and colocalized at the transverse cell interface, as indicated in the high magnification images (Fig. 1 *G* and *H*). Fluorescence signal intensity analysis further supports that VAP27-1 and SCAR2 are highly enriched in the apical/basal plasma membrane, with a higher axial-to-lateral signal ratio on the PM. In contrast, the signal ratio of FM4-64 labeled PM is close to 1.0, indicating a nonpolarized localization (Fig. 1*I*). In addition, there was an enrichment of SCAR2 at the cell corners, which may be related to stronger local actin polymerizing activity and root cell elongation (*SI Appendix*, Fig. S2); a similar behavior has been reported for other SCAR/WAVE subunits (e.g., BRK1 and NAP1) (12, 46).

SCAR2 and VAP27 Regulate Primary Root Growth and Affect the Cytokinetic Activity of Root Meristems. To gain further insight into the biological relevance of the SCAR and VAP27 interaction, we performed phenotypical analysis using the *scar1234* quadruple mutant (T-DNA insertional mutant of SCAR1, 2, 3, and 4) and the *vap27-1346* quadruple mutant (CRISPR knock-out of four VAP27 genes, VAP27-1, -3, -4, and -6). These lines were obtained from previous publications and validated as functional knock-out

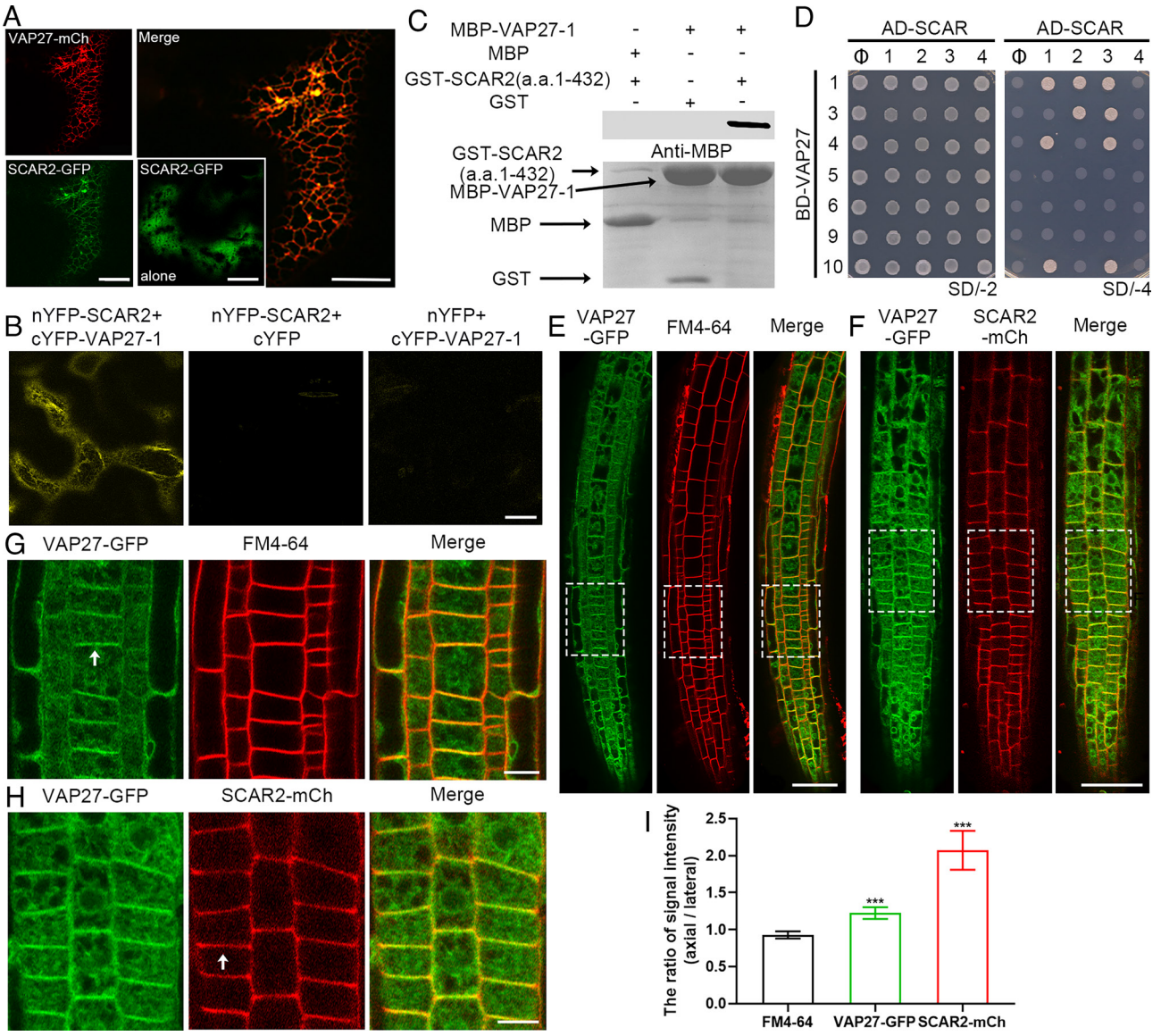

Fig. 1. SCAR2 interacts with VAP27 proteins and exhibits polarized localization at the transverse cell plate. (*A*) In *N. benthamiana* leaf epidermal cells, VAP27-mCh recruits GFP-SCAR2 to the ER membrane when coexpressed. (Scale bar, 20 μm.) (*B*) BiFC assays in *N. benthamiana* show that SCAR2 interacts with VAP27-1 on the ER. An empty vector is used as a negative control. (Scale bar, 20 μm.) (*C*) In vitro pull-down assay confirmed the interaction between MBP-VAP27-1 and a GST-SCAR2 truncation. The top panel shows the pull-down results, where VAP27-1 is detected in the presence of GST-SCAR2 (a.a. 1 to 432) using an anti-MBP antibody; the bottom panel shows the total protein stained by Coomassie brilliant blue. MBP protein and GST protein were used as negative controls (left and middle lanes). Arrows indicate specific bands of purified proteins. (*D*) A one-on-one yeast two-hybrid screen revealed conserved interactions between the SCAR and VAP27 families. Transformed yeast cells were cultured on SD/-Trp-Leu (SD/-2) or SD/-Trp-Leu-His-Ade (SD/-4) medium, respectively. (*E–H*) VAP27-GFP colocalized with FM4-64 and SCAR2-mCh in transgenic *Arabidopsis* roots at the transverse cell interface (arrows). Scale bar, 50 μm in (*E* and *F*) and 10 μm in (*G* and *H*). The signal intensity of FM4-64, VAP27, and SCAR2 at the axial/lateral cell membrane was quantified as in (*I*). Quantification was performed using at least 30 cells from 5 roots. Two-tailed *t* test, ***$P < 0.001$.

mutants (46, 47). We mainly focused on root tissue where SCAR2 and VAP27 are coexpressed and found the primary root of both *scar1234* and *vap27-1346* mutant seedlings are significantly shorter than the wild type (Fig. 2 *A* and *B*). Such a defect was likely caused by a reduced number of meristem cells and a shorter meristem region (Fig. 2 *C–J*). To further determine the function of SCAR and VAP27 in the root meristem, 3-day-old seedlings were stained with DAPI and 5-ethynyl-20-deoxyuridine (EdU), which selectively labels the nucleus of newly divided cells. Image quantification of the EdU/DAPI ratio showed that the number of newly divided cells was significantly reduced in the *scar1234* and *vap27-1346* mutants, consistent with the observation of reduced meristem size (Fig. 2 *K* and *L*). Both *scar1234* and *vap27-1346* also show similar defects in pavement cell morphogenesis (*SI Appendix*, Fig. S3), a process regulated by the actin cytoskeleton.

In addition, the seedlings of *vap27-1346* mutants also show a twisted root phenotype (Fig. 2*B*). Therefore, the root epidermal cells of *vap27-1346* were studied in-depth using propidium iodide (PI) staining (Fig. 2*M*), and the results suggested that the cell organization is different. In the wild-type, the transverse cell wall is almost perpendicular to the growth direction; however, their orientations are highly variable in the *vap27-1346* mutant (Fig. 2*N*), indicating the direction of cell division is likely affected. Given these findings and the conserved function of SCAR in actin nucleation and branching, we hypothesize that the root phenotype observed in *vap27-1346* is likely related to defects in the assembly of actin filaments. To test this hypothesis, wild-type *Arabidopsis* seedlings were germinated on 1/2 MS medium containing a low concentration of an actin polymerization inhibitor, latrunculin B (Lat B). Similarly, shorter primary roots, reduced meristem size, and disorganized cell

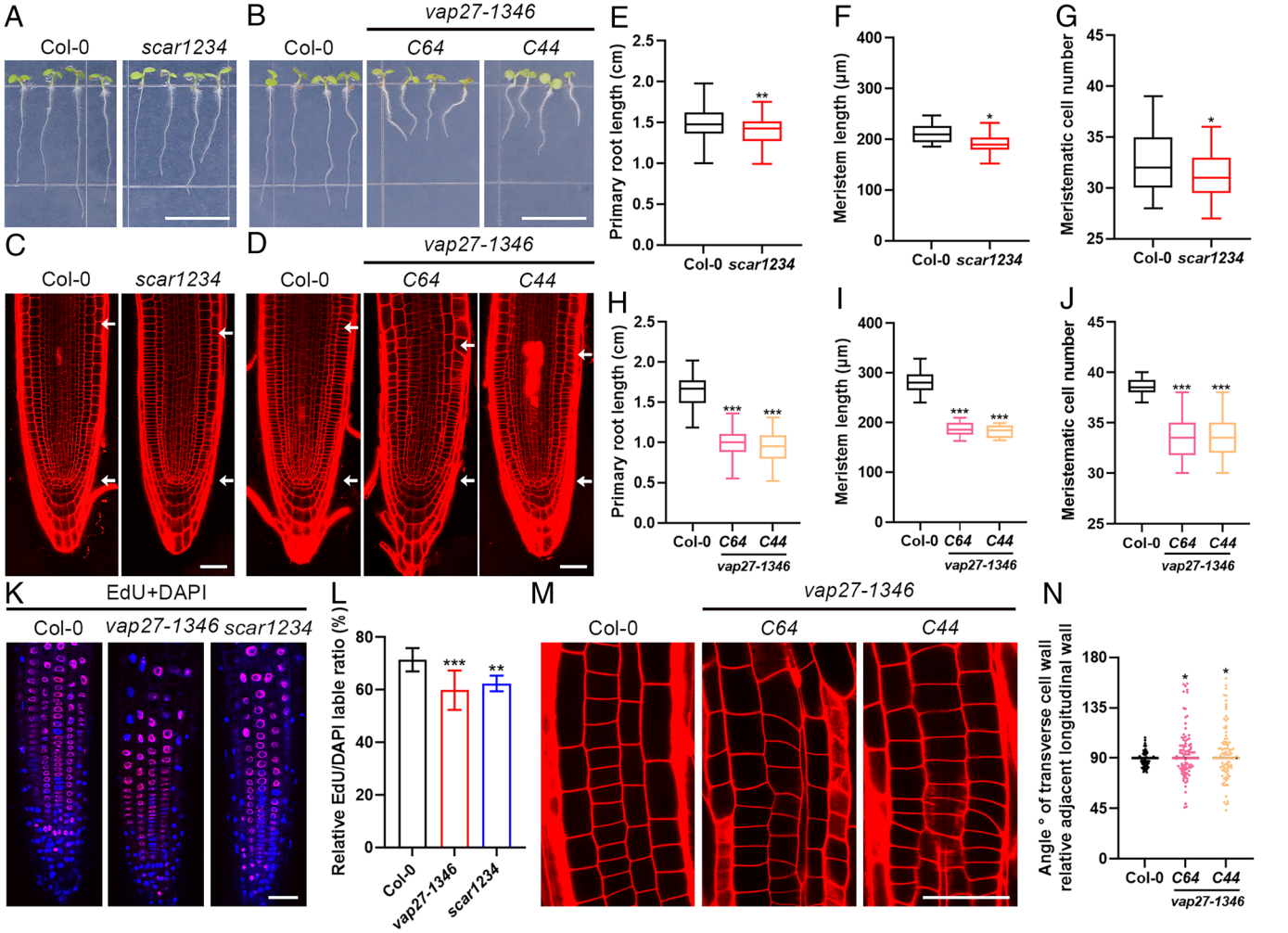

Fig. 2. The quadruple mutant of *vap27-1346* and *scar1234* exhibit root growth defects. (*A–D*) Images of Col-0, *scar1234,* and *vap27-1346* seedlings (5 dpg) indicate that the mutation of SCAR and VAP27 resulted in similar root defects. Roots were stained with PI and imaged at 5 dpg. White arrows indicate the quiescent center (QC) and root meristem boundary. (*E–J*) Quantifications of the primary root length, root meristem length and meristematic cell number of seedlings in (*A–D*). Scale bar, 1 cm in (*A* and *B*), and for each dataset, n >50. Scale bar, 50 μm in (*C* and *D*), n ≥ 10 roots. Student's *t* test, **P* < 0.05, ***P* < 0.01, ****P* < 0.001. (*K–L*) The EdU and DAPI staining reveals that *vap27-1346* and *scar1234* exhibit cell division defects. (Scale bar, 50 μm.) The percentage of EdU labeled nuclei in root meristem was quantified in Col-0, *scar1234*, and *vap27-1346* (as in *L*). n ≥ 10, two-tailed *t* test, **P* < 0.05, ***P* < 0.01, ****P* < 0.001. (*M* and *N*) The organization of root epidermal cells is more disordered in the *vap27-1346* mutant, as indicated by the angles of the transverse cell plates, which show higher variability in the VAP27 mutant. Roots were stained with PI and imaged at 5 dpg. (Scale bar, 50 μm.) For each dataset, n = 100, two-tailed *t* test, **P* < 0.05.

division patterns were also observed (*SI Appendix*, Fig. S4 *A–F*), indicating the root phenotype in the *vap27-1346* mutant is likely to be actin cytoskeleton related. Actin density at the division plane is significantly reduced after the mild Lat B treatment (200 nM), while the ER density (as indicated by VAP27-mCherry) hardly changes (*SI Appendix*, Fig. S4 *G–I*).

Taken together, these results indicate that the interaction between the actin nucleation factor SCAR and the EPCS protein VAP27 is likely essential for root growth and meristem maintenance. Knocking out the VAP27 proteins may inhibit actin assembly (mimicking the phenotype of Lat B treatment), ultimately affecting cell division and root meristem defect. As the VAP27 and SCAR mutants showed similar phenotypes, we speculated that both proteins are likely to act in a shared pathway.

The Cortical ER Network and ER–PM Interaction are Involved in Cell Plate Formation. Previous studies found that the ER membrane is highly enriched at the division plane and the developing cell plates (42), but the exact function of the ER in plant cytokinesis is unknown. In plants, the ER–PM tethering protein VAP27 is also associated with the cytoskeleton network at the ER–PM contact sites (15, 16, 20, 21, 24, 25, 48). Given the involvement of VAP27 in *Arabidopsis* root growth and meristematic cell patterning (Fig. 1 *F* and *G*), we speculated that the ER network and ER–PM interaction could be involved in cell division and cell plate formation. To address this question, we generated stable *Arabidopsis* lines expressing an artificial EPCS marker (MAPPER-GFP) under the control of a ubiquitin promoter (49). In root meristems, both MAPPER-GFP and VAP27-GFP showed polarized localization at the transverse cell interface (*SI Appendix*, Fig. S5 *A–D*), and their signal strongly overlapped with FM4-64. Similar behavior is not very prominent in GFP-HDEL (a general ER marker; *SI Appendix*, Fig. S5 *E* and *F*) expressing lines (50), suggesting that the ER signal enrichment at the cell interface likely requires ER–PM tethering.

To better understand the differential behaviour between the ER and EPCS markers, we studied the late cytokinesis process using different transgenic lines. FM4-64 is employed as a cell plate marker as it labels newly synthesized membrane at the division plane. In contrast to the localization of GFP-HDEL (Fig. 3*A*), the signals of EPCS markers (MAPPER-GFP, VAP27-GFP) are more enriched at the cell plate (*SI Appendix*, Fig. S6), suggesting

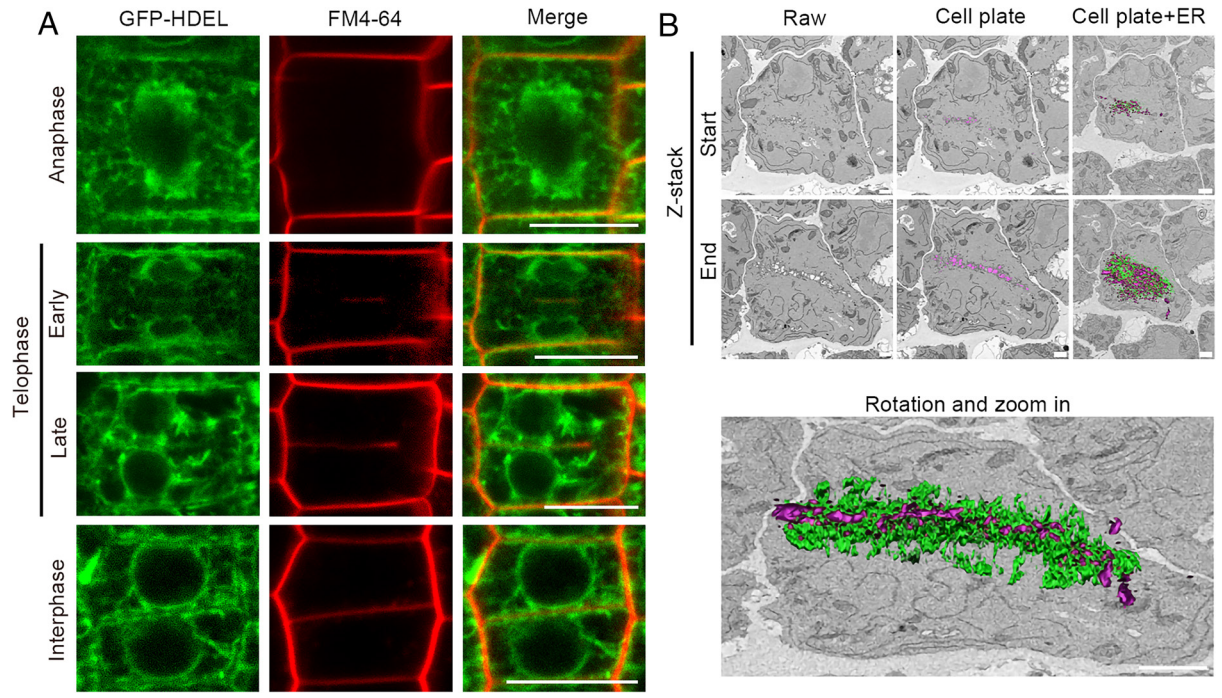

Fig. 3. ER is enriched at the cell plate. (*A*) The ER network (GFP-HDEL labeled) is enriched at the cell division plane at different stages. (Scale bar, 10 μm.) (*B*) SBEM images of a dividing cell from *Arabidopsis* root meristem. The ER membrane is green, and the cell plate/tubular network is magenta. (Scale bar, 2 μm.) FM4-64 is used to label PM and cell plate membranes during cytokinesis. (Scale bar, 10 μm.)

ER–PM interactions are likely very abundant at the cell plate region. The ER labeling at the cell plate gradually increases during the telophase, reaching its highest point as it matures (Fig. 3*A*). Serial-block face SEM (SBEM) studies further confirmed this observation at the ultrastructural level, with massive accumulations of ER membrane associated with both sides of the cell plate (Fig. 3*B* and Movie S1). In summary, these results indicate that the ER membrane is closely associated with the cell plate, and this specific membrane interaction probably involves ER–PM tethering factors (e.g., VAP27, *SI Appendix*, Fig. S6*B*). Therefore, we investigated the function of the VAP27–SCAR2 interaction and ER–actin association during cytokinesis.

VAP27 Recruits SCAR to Regulate Cell Plate Expansion and Actin Assembly. According to the subcellular localization and phenotypic study of VAP27-1 and SCAR2, we speculated that both proteins might contribute to root meristem maintenance through regulating cytokinesis. Confocal microscopy observation revealed that VAP27 was initially enriched at the cell division plane since the late anaphase (*SI Appendix*, Fig. S7). In contrast, the signal of SCAR2 was more evident from the telophase (Fig. 4*A*). Further quantification confirmed that the fluorescence intensity of SCAR2 showed a gradual increase at the late telophase. In contrast, the VAP27 signal increases before that (Fig. 4 *A* and *B*). Given the previously demonstrated interaction between VAP27-1 and SCAR2, it is likely that VAP27 accumulates at the division plane first and then recruits SCAR2 sequentially. We tested this hypothesis by studying SCAR2-mCh in different genetic backgrounds. In the *vap27-1346* mutant, the polarized distribution of SCAR2 is affected significantly (Fig. 4*C*). The fluorescence intensity of SCAR2-mCh at axial and lateral PM was quantified. The result suggested that the SCAR2 signal does not accumulate on the transverse cell interface (Fig. 4*D*), likely due to the abolished interaction with VAP27, so it cannot be efficiently recruited to the new division plane. Furthermore, the ER fluorescence intensity is significantly reduced in the *vap27-1346* mutant (Fig. 4*E*); this observation is confirmed by the signal ratio of GFP-HDEL at the division plane and cytoplasm (Fig. 4*F*). Meanwhile, the TEM images showed a reduction in the density of ER surrounding the cell plate (Fig. 4*G*).

The actin cytoskeleton is important for cell division and cell plate directional expansion; it is enriched alongside the preprophase band (PPB) and defines the cell division plane with microtubules (51–53). In the *Arabidopsis* root, F-actin accumulated at the apical–basal plasma membrane, which might determine cell polarity during cell division (54). As SCAR2 promotes actin elongation and branching, transgenic *Arabidopsis* lines expressing SCAR2-mCh or VAP27-1-mCh were crossed with an actin marker line (GFP-Lifeact) to study the behaviour of actin and ER during cytokinesis. As the cell plate expands at telophase, there is a significant accumulation of actin bundles at the division plane, together with VAP27 and SCAR2 (Fig. 5 *A* and *B*), whereas the signal of VAP27 is enriched at the leading edges in particular (Fig. 5*B*). In both *vap27-1346* and *scar1234* mutant, the fluorescence intensity of actin was significantly reduced at the cell division plane and transverse cell interface of root epidermal cells (Fig. 5 *C*–*F*). In addition, we measured the maximum length of cell plates at different time points and calculated the cell plate expansion rate as micrometer per minute. The results showed that the growth rate of cell plates in the *vap27-1346* is significantly slower than Col-0 (Fig. 5 *G* and *H* and Movies S2 and S3).

Taken together, these results suggest that VAP27 modulates SCAR and actin recruitment, forming a VAP27–SCAR–actin macromolecular complex that facilitates ER–PM interaction and actin nucleation at the division plane, ultimately affecting the speed and direction of cell plate expansion and root development.

The Function of SCAR2 Requires VAP27 Interaction. According to the protein interaction results and mutant phenotype studies, it is likely that VAP27 and SCAR2 regulate cell division and root development in a coordinated way; therefore, we then addressed whether the interaction of VAP27 is essential for SCAR2 function.

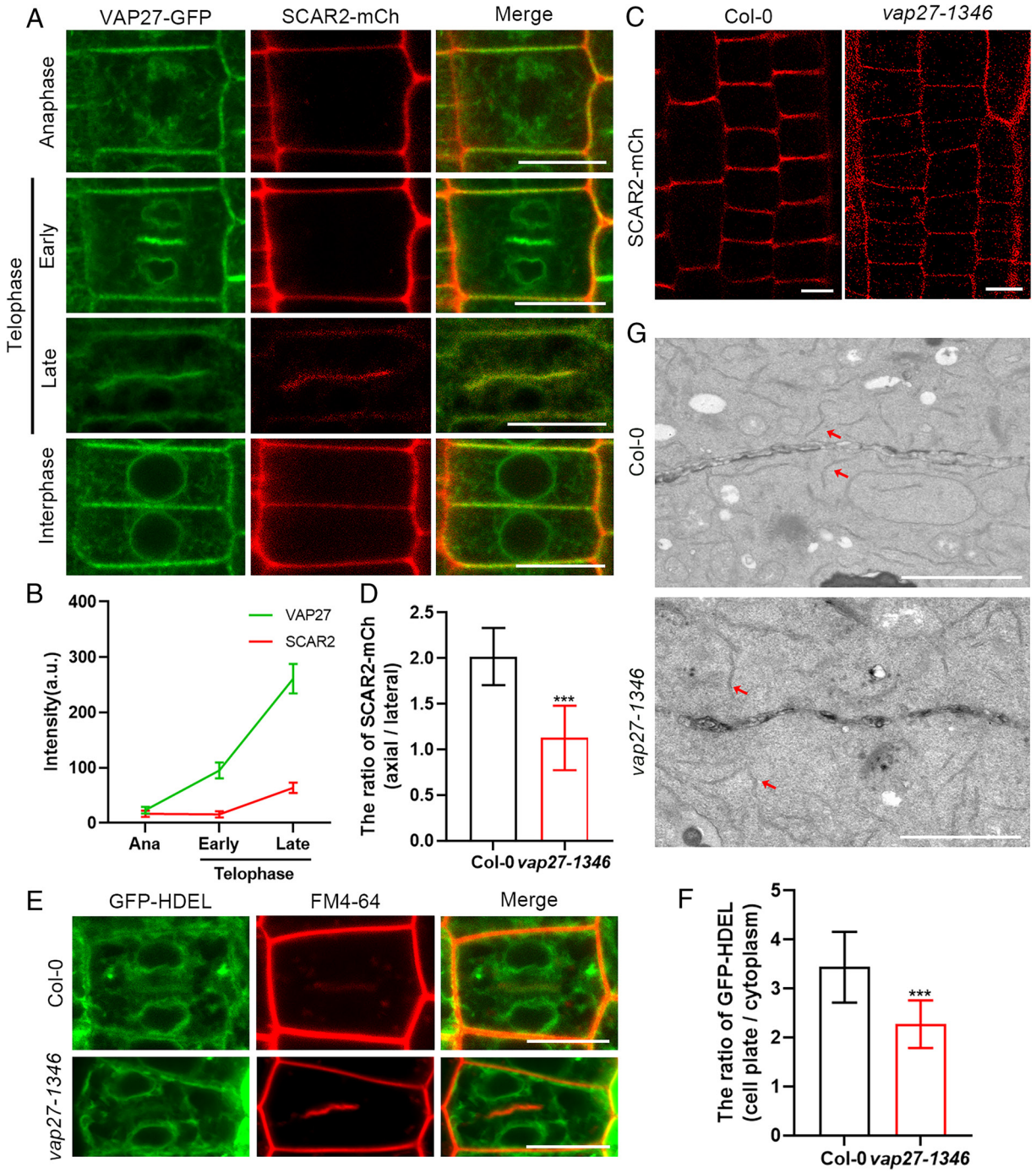

Fig. 4. VAP27 regulates the accumulation of SCAR2 and ER membrane to the division plane. (*A* and *B*) Cells from transgenic *Arabidopsis* root meristem expressing VAP27-GFP and SCAR2-mCh. Both fusion proteins are recruited to the cell plate, and the transverse cell interfaces during cytokinesis, but the recruitment of VAP27 appears earlier than SCAR2. The relative signal intensity (signals from cell plate/cytoplasm) of VAP27-GFP and SCAR2-mCh at the early and late telophase was quantified in (*B*). (Scale bar, 10 μm.) At least 10 cells were analyzed per stage. (*C*) The localization of SCAR2-mCh in root meristem cells is affected in the *vap27-1346* mutant. (Scale bar, 10 μm.) (*D*) The quantification of SCAR2-mCh signals at the axial/lateral cell membrane of the Col-0 and *vap27-1346* mutant, polarized localization of SCAR2 at the transverse cell interfaces is perturbed in the absence of VAP27. n > 30, two-tailed *t* test, ***$P < 0.001$. (*E* and *F*) Images of transgenic *Arabidopsis* root meristem cells expressing GFP-HDEL; signals of the ER membrane at the division plane (late-telophase) are reduced significantly in the *vap27-1346* mutant. The ratios of the ER labeling at the cell division plane and cytoplasm are shown in (*E*). FM4-64 is used to label cell membranes. (Scale bar, 10 μm.) At least 10 cells were analyzed for each stage. (*G*) TEM images suggest that the ER membranes at the cell plate region are reduced in *vap27-1346* mutant at 3 dpg. (Scale bar, 2 μm.)

First, we generated a number of SCAR2 truncations to determine the motif required for the interaction. Through a yeast two-hybrid assay, we found the N-terminal sequence of SCAR2 (a.a. 1 to 432) is sufficient for VAP27 interaction, and subsequent truncation of $SCAR2^{1\text{-}432}$ further narrowed this interacting motif to a.a. 340 to 432 (Fig. 6 *A* and *B*), which contains three linear interactive peptides (LIPs) as predicted by MobiDB (55). It has been shown that the LIP peptides are likely involved in protein interactions (56). In yeast and animals, the FFAT motif (consecutive phenylalanines in an acidic tract) are recognized by VAP through its major sperm domain (MSD) (22, 56, 57). Using the VAP interactome prediction program (56), we have found a FFAT-like motif (LTSEADNYVDAPAT) within the LIP1 peptide (Fig. 6*C*). Therefore, we suspected that the LIP1 motif (a.a. 357 to 388) could be essential for the VAP27

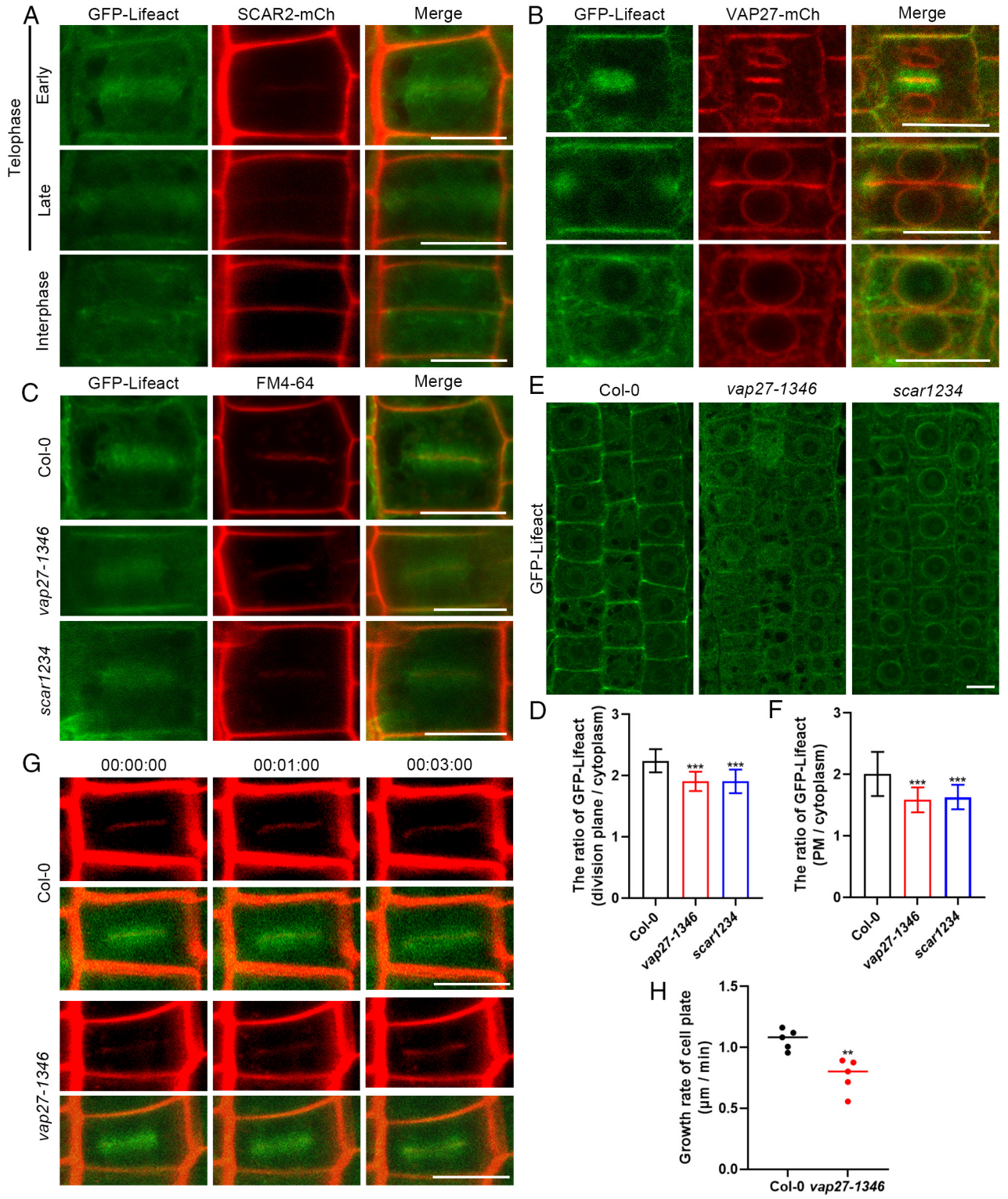

Fig. 5. VAP27 and SCAR2 proteins regulate actin accumulation at the division plane and transverse cell interface. (*A* and *B*) In *Arabidopsis* root meristem cells, GFP-Lifeact labeled actin filaments form actin patches and colocalize with SCAR2-mCh or VAP27-mCh labeled cell plates. (Scale bar, 10 μm.) (*C* and *D*) Images of transgenic *Arabidopsis* root meristem cells expressing GFP-Lifeact, signals of the actin filaments at the division plane (late-telophase) are reduced significantly in the *vap27-1346* mutant. The ratios of the actin labeling at the cell division plane and cytoplasm are shown in (*D*). FM4-64 is used to label cell plates. (Scale bar, 10 μm.) At least 10 cells were analyzed for each stage. (*E* and *F*) Images of transgenic *Arabidopsis* root epidermal cells expressing GFP-Lifeact, signals of the actin filaments at the transverse cell interface are reduced significantly in the *vap27-1346* and *scar1234* mutant. At least 30 cells from 5 roots. Two-tailed *t* test, ***$P <$ 0.001. (*G* and *H*) Time-series imaging reflected a significantly slower growth rate of the cell plate in the *vap27-1346* mutant than in the wild type. FM4-64 is used to label cell plates. Actin filaments are labeled with green fluorescence. n = 5, two-tailed *t* test, **$P < 0.01$. (Scale bar, 10 μm.) Cell plates with an initial length at 7 to 8 μm were selected and imaged for three minutes.

interaction in plants. Indeed, yeast two-hybrid and BiFC assays confirmed that deletion of LIP1 (SCAR2$^{\Delta LIP1}$) prevents VAP27-1 interaction (Fig. 6 *D* and *E*). Meanwhile, the interactions between LIP1 and VAP27-1 have been further validated by AlphaFold3 protein docking prediction (58) (*SI Appendix*, Fig. S8 *A* and *B*) and in vitro pull-down assays (*SI Appendix*, Fig. S8*C*).

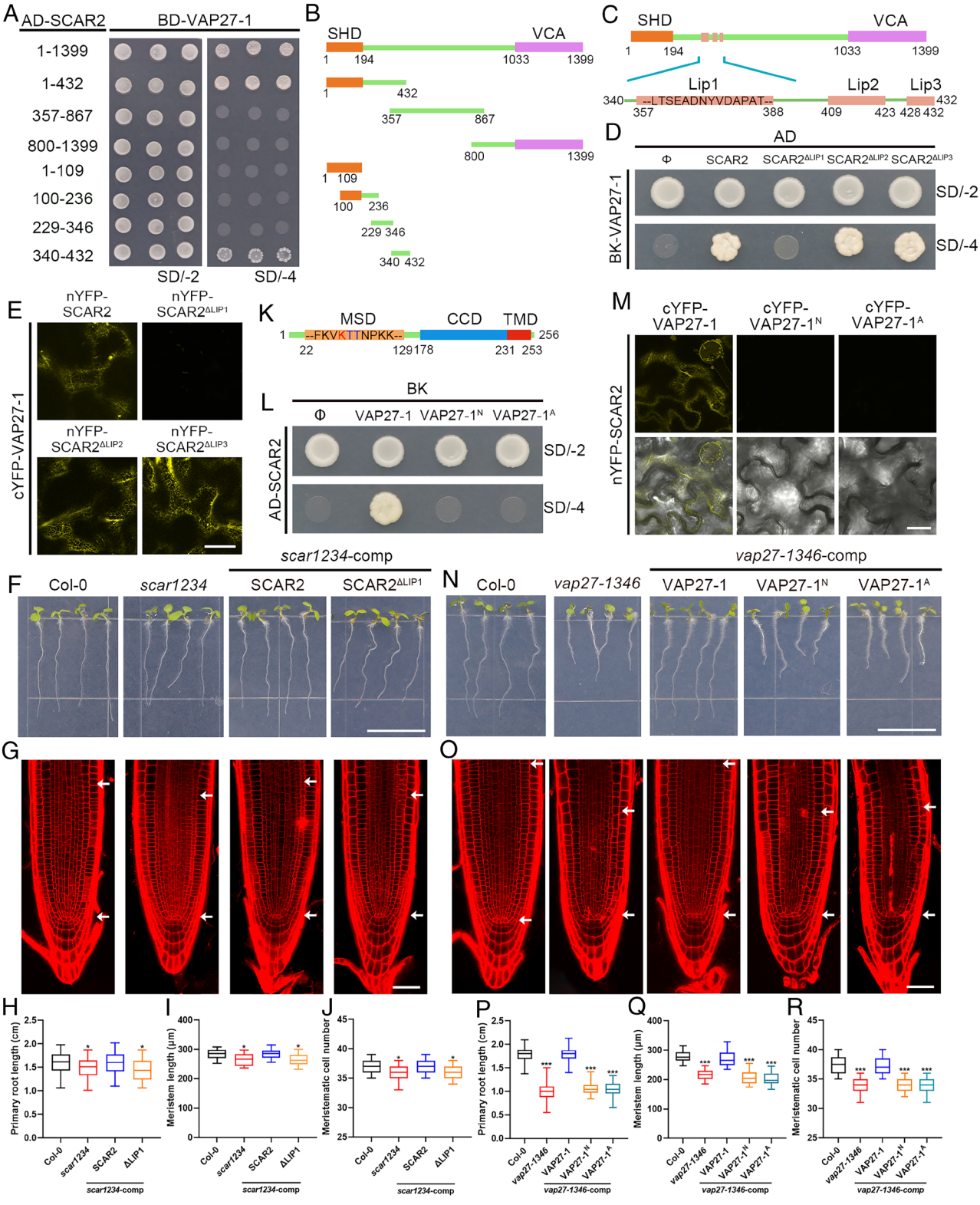

Fig. 6. Functional complementation studies indicate the interaction between SCAR2 and VAP27-1 is essential for their function. (*A* and *B*) Yeast two-hybrid assay suggests the C-terminal sequence of SCAR2 (a.a. 340 to 432) is required for VAP27 interaction. (*C*) Three predicted linear interacting peptides (LIP) are found between a.a. 340 to 432 on SCAR2, and the LIP1 sequence contains an FFAT-like motif. (*D* and *E*) Y2H and BiFC assays show that SCAR2 without LIP1 sequence (SCAR2$^{\Delta LIP1}$) fails to interact with VAP27-1. (Scale bar, 20 μm.) (*F* and *G*) Gene complementation assay suggests that the expression of SCAR2$^{\Delta LIP1}$ (pSCAR2:SCAR2$^{\Delta LIP1}$-HA/*scar1234,* denoted as *scar1234-comp*$^{\Delta LIP1}$) cannot fully complement the root phenotype of the *scar1234* mutant, suggesting VAP27-1 interaction is important for SCAR2 function. (*H–J*) Quantifications of primary root length, meristem length, and meristematic cell number in (*F* and *G*). (*K*) The conserved lysine (K) and Threonine (T) residues within the major sperm domain (MSD) are likely responsible for interacting with the FFAT motif. (*L* and *M*) Y2H and BiFC assays demonstrate that these conserved residues are critical for the interactions between SCAR2 and VAP27-1. (Scale bar, 20 μm.) (*N* and *O*) The expression of full-length VAP27-1 (pVAP27-1:VAP27-1-HA) complements root phenotypes of the *vap27-1346* mutant, while the VAP27-1^{N} (pVAP27-1:VAP27-1^{N}-HA) and VAP27-1^{A} (pVAP27-1:VAP27-1^{A}-HA) point mutant fails to complement the mutant phenotype. (*P–R*) Quantifications of primary root length, meristem length, and meristematic cell number in (N-O). Roots were stained with PI and imaged at 5 dpg. White arrows indicate the QC and root meristem boundary. Scale bar, 1 cm in (*F* and *N*) and 50 μm in (*G* and *O*), respectively. For each dataset in (*H* and *P*), n ≥ 50. For each dataset in (*I*, *J*, *Q*, and *R*), n ≥ 10, two-tailed *t* test, **P* < 0.05, ***P* < 0.01, ****P* < 0.001.

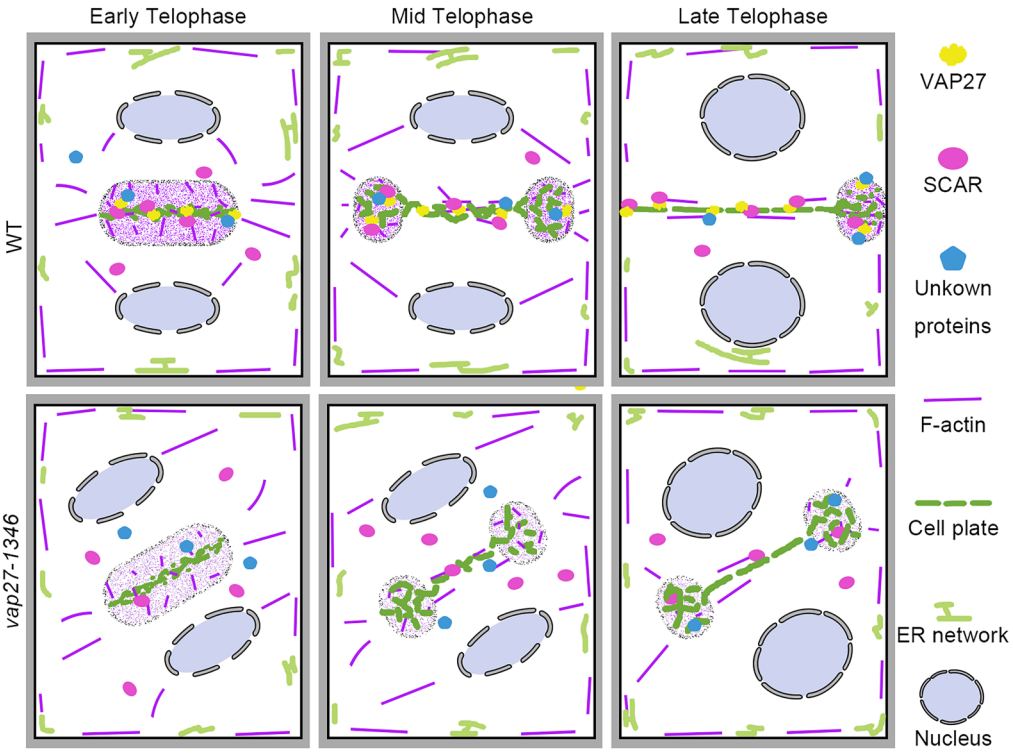

Fig. 7. Schematic illustration of VAP27-SCAR regulated ER–PM–Actin interaction during cytokinesis. In wild-type cells, VAP27 is localized to the ER and ER–PM contact sites, and it is significantly enriched on the cell division plane. As the cell divides, VAP27 gradually accumulates at the cell plate region, where it recruits the SCAR/WAVE complex to promote actin nucleation and cell plate expansion. In the *vap27-1346* mutant, SCAR cannot be recruited to the cell plate to activate actin nucleation, resulting in abnormal cell plate expansion rate, orientation, and assembly.

We transformed the pSCAR2:SCAR2-HA and pSCAR2:SCAR2$^{\Delta LIP1}$-HA construct into the *scar1234* quadruple mutant to test whether the LIP1 domain is required for SCAR2 function during cell division. Full-length SCAR2 could complement the meristem and root growth phenotype of the *scar1234* mutant. However, gene complementation using SCAR2$^{\Delta LIP1}$ cannot do the same (Fig. 6 *F–J*), suggesting that the activity of SCAR2 is dependent on the VAP27 interaction, which recruits it to the ER membrane (Fig. 1*A*). A similar experiment was also performed with VAP27-1. Previous studies indicated that a lysine residue (a.a. 58) and two threonine residues (a.a. 59 to 60) are indispensable for VAP27-1 to interact with other proteins (22). Therefore, we substituted the lysine for asparagine (VAP27-1^{N}) and the threonine for alanine (VAP27-1^{A}). The mutated VAP27-1 was tested for interaction with SCAR2 via Y2H and BiFC assays, and the results demonstrated that the mutant VAP27-1 could not interact with SCAR2 (Fig. 6 *K–M*). Not surprisingly, both VAP27-1^{N} and VAP27-1^{A} mutant (driven by its native promoter) cannot complement the root phenotype of the *vap27-1346* quadruple mutant, consistent with the conclusion that VAP27–SCAR interaction is important for their function and root development (Fig. 6 *N–R*).

Discussion

Collectively, the ER–PM tethering protein VAP27 recruits ER and SCAR to the cell plate to produce a plant-specific configuration of cytoskeleton ER–PM interaction. Using multiple approaches, we showed that the SCAR of the SCAR/WAVE complex interacts with VAP27. This macromolecular complex supports cell plate orientation and regulates meristem cell maintenance and root development. In the absence of VAP27, we observed that the contact between the ER membrane and the cell plate is reduced, consequently affecting SCAR recruitment and actin filament formation (Fig. 7).

The position and direction of cell plate formation determine the dimensions of cell proliferation and organ morphology. Previously, numerous studies reported that microtubules are necessary for the synthesis of cell plates (26, 52, 59). Nevertheless, the expansion of the phragmoplast and cell plate are also influenced by actin polymerization inhibitors (42). At the PPB formation stage, actin polymerization and rearrangement generate forces on the PPB and define the position of the cell division plane (42–44), ultimately influencing the formation of new cells (31, 52, 53, 60, 61). Moreover, myosins are localized to the edge of the phragmoplast and the cell division site (30–32), where they play a role in ensuring the correct orientation of the cell plate and the accurate recognition of the fusion site on the parent cell (32, 33, 53). This reflects the involvement of actin in determining the direction of cell proliferation, which is crucial for plant growth and morphogenesis. VAP27 is a protein that localizes at the ER membrane and ER–MCS; it also accumulates at the cell division plane where the cell plate is formed (Fig. 1*E*). Actin likely assembles into short bundles at the phragmoplast, forming the scaffold with microtubules and other proteins to direct vesicle trafficking and cell plate expansion (30). In this study, we show the interaction between VAP27 and SCAR at the cell plate (Fig. 4*A*). Further analysis using various mutant and transgenic lines suggest that VAP27 is required for the polarized localization of SCAR2. In the *vap27-1346* mutant, the SCAR2 localization and actin cytoskeleton accumulation at the division plane and transverse cell–cell interface are affected, suggesting VAP27 is able to recruit SCAR to regulate actin density. This process is likely involved in cell plate expansion and directional growth.

In addition to the function of SCAR recruitment and actin nucleation, the VAP27-regulated ER–PM interaction is likely to

be involved in many biological activities during cell division. It has been reported that many ER tubules traverse the cell plate during its formation, eventually forming plasmodesmata (35–38), which provide cytoplasmic and membrane continuity between adjacent cells, facilitating direct communication and transport of molecules between cells. VAP27 has been reported to partially colocalize with plasmodesmata (20, 24), and here, we show the accumulation of VAP27 on the cell plate (Fig. 4*A*), indicating a possible function of VAP27 in plasmodesmata biogenesis. In addition, VAP27 bridges the ER with endocytic membranes and contributes to endocytic trafficking events, which are essential for cell plate maturation and fusion with the parent cell (51).

In summary, the complex assembled by VAP27 recruits SCAR and facilitates ER–PM–actin interaction at the cell plate, which enables the guidance of cell plate expansion and orientation. In the future, it will be intriguing to study how the functions of the ER, actin and microtubules are coordinated during cytokinesis. The establishment of ER–PM connections could be essential, as the ER–PM contact sites are the place where actin and microtubules converge.

Materials and Methods

Detailed *Materials and Methods* are provided in *SI Appendix*. These include details about plant materials and molecular cloning, confocal microscopy and image analysis, yeast two-hybrid assays, protein purification and in vitro pull-down assays, light microscopy and 5-ethynyl-20-deoxyuridine (EdU) staining, election microscopy, serial-block face scanning electron microscopy and data reconstructions, latrunculin B treatment, and statistical analysis.

Data, Materials, and Software Availability. All study data are included in the article and/or supporting information.

ACKNOWLEDGMENTS. The project was supported by NSFC Grants (92254307, 32261160371), Fundamental Research Funds for the Central Universities (2662023PY011), Young Scientist Fostering Funds for the National Key Laboratory for Germplasm Innovation and Utilization of Horticultural Crops (Horti-PY-2023-001), Science and Technology Project of Hubei Province (2024AFE005) to P.W., a China Postdoctoral Science Foundation Grant (2022M721271) to J.Z., and a BBSRC Grant, BBC516601/1, to P.J.H. We thank the support from microscopy core facilities of the College of Horticulture & Forestry Sciences, Huazhong Agricultural University. We thank Prof. Elison B. Blancaflor and Dr. Sabrina Chin (Noble Research Institute) for sharing the SCAR2-mCherry transgenic lines and the *scar1234* mutant. We thank Dr Weibing Yang (CEMPS) for the pUBQ: GFP-Lifeact transgenic line. We thank Dr. Patrick Duckney (Durham University) and Dr. Tong Zhang (HZAU) for their help and advice throughout the project.

Author affiliations: [a]National Key Laboratory for Germplasm Innovation and Utilization of Horticultural Crops, College of Horticulture and Forestry Sciences, Huazhong Agricultural University, Wuhan 430070, China; [b]Hubei Hongshan Laboratory, Wuhan 430070, China; [c]School of Biological and Medical Sciences, Oxford Brookes University, Oxford OX3 0BP, United Kingdom; [d]Department of Biosciences, Durham University, Durham DH1 3LE, United Kingdom; [e]College of Horticulture and Landscape Architecture, Yangzhou University, Yangzhou 225009, China; and [f]Biosciences, University of Exeter, Exeter EX4 4QD, United Kingdom

1. T. D. Pollard, Regulation of actin filament assembly by Arp2/3 complex and formins. *Annu. Rev. Biophys. Biomol. Struct.* **36**, 451–477 (2007).
2. L. Xu, L. Cao, J. Li, C. J. Staiger, Cooperative actin filament nucleation by the Arp2/3 complex and formins maintains the homeostatic cortical array in Arabidopsis epidermal cells. *Plant Cell* **36**, 764–789 (2024).
3. M. Frank *et al.*, Activation of Arp2/3 complex-dependent actin polymerization by plant proteins distantly related to Scar/WAVE. *Proc. Natl. Acad. Sci. U. S. A.* **101**, 16379–16384 (2004).
4. C. Zhang *et al.*, Arabidopsis SCARs function interchangeably to meet actin-related protein 2/3 activation thresholds during morphogenesis. *Plant Cell* **20**, 995–1011 (2008).
5. J. F. Uhrig *et al.*, The role of Arabidopsis SCAR genes in ARP2-ARP3-dependent cell morphogenesis. *Development* **134**, 967–977 (2007).
6. S. Chin *et al.*, Spatial and temporal localization of SPIRRIG and WAVE/SCAR reveal roles for these proteins in actin-mediated root hair development. *Plant Cell* **33**, 2131–2148 (2021).
7. C. Liu *et al.*, An actin remodeling role for Arabidopsis processing bodies revealed by their proximity interactome. *EMBO J.* **42**, e111885 (2023).
8. M. R. Facette *et al.*, The SCAR/WAVE complex polarizes PAN receptors and promotes division asymmetry in maize. *Nat. Plants* **1**, 14024 (2015).
9. C. Zhang *et al.*, The endoplasmic reticulum is a reservoir for WAVE/SCAR regulatory complex signaling in the Arabidopsis leaf. *Plant Physiol.* **162**, 689–706 (2013).
10. M. Yanagisawa, C. Zhang, D. B. Szymanski, ARP2/3-dependent growth in the plant kingdom: SCARs for life. *Front. Plant Sci.* **4**, 166 (2013).
11. J. Dyachok *et al.*, SCAR mediates light-induced root elongation in Arabidopsis through photoreceptors and proteasomes. *Plant Cell* **23**, 3610–3626 (2011).
12. P. Wang, C. Richardson, C. Hawes, P. J. Hussey, Arabidopsis NAP1 regulates the formation of autophagosomes. *Curr. Biol.* **26**, 2060–2069 (2016).
13. J. Martinek *et al.*, ARP2/3 complex associates with peroxisomes to participate in pexophagy in plants. *Nat. Plants* **9**, 1874–1889 (2023).
14. C. Pain, F. Tolmie, S. Wojcik, P. Wang, V. Kriechbaumer, intER-ACTINg: The structure and dynamics of ER and actin are interlinked. *J. Microsc.* **291**, 105–118 (2023).
15. J. Zang, V. Kriechbaumer, P. Wang, Plant cytoskeletons and the endoplasmic reticulum network organization. *J. Plant Physiol.* **264**, 153473 (2021).
16. P. Wang, T. J. Hawkins, P. J. Hussey, Connecting membranes to the actin cytoskeleton. *Curr. Opin. Plant Biol.* **40**, 71–76 (2017).
17. P. Cao, L. Renna, G. Stefano, F. Brandizzi, SYP73 anchors the ER to the actin cytoskeleton for maintenance of ER integrity and streaming in Arabidopsis. *Curr. Biol.* **26**, 3245–3254 (2016).
18. P. Wang, P. J. Hussey, Interactions between plant endomembrane systems and the actin cytoskeleton. *Front. Plant Sci.* **6**, 422 (2015).
19. I. Sparkes, J. Runions, C. Hawes, L. Griffing, Movement and remodeling of the endoplasmic reticulum in nondividing cells of tobacco leaves. *Plant Cell* **21**, 3937–3949 (2009).
20. P. Wang, C. Hawes, P. J. Hussey, Plant endoplasmic reticulum-plasma membrane contact sites. *Trends Plant Sci.* **22**, 289–297 (2017).
21. S. Sun *et al.*, Stay in touch with the endoplasmic reticulum. *Sci. China Life Sci.* **67**, 230–257 (2024).
22. C. J. Loewen, T. P. Levine, A highly conserved binding site in vesicle-associated membrane protein-associated protein (VAP) for the FFAT motif of lipid-binding proteins. *J. Biol. Chem.* **280**, 14097–14104 (2005).
23. K. Bürstenbinder *et al.*, Arabidopsis calmodulin-binding protein IQ67-domain 1 localizes to microtubules and interacts with kinesin light chain-related protein-1. *J. Biol. Chem.* **288**, 1871–1882 (2013).
24. P. Wang *et al.*, The plant cytoskeleton, NET3C, and VAP27 mediate the link between the plasma membrane and endoplasmic reticulum. *Curr. Biol.* **24**, 1397–1405 (2014).
25. J. Zang *et al.*, A novel plant actin-microtubule bridging complex regulates cytoskeletal and ER structure at ER-PM contact sites. *Curr. Biol.* **31**, 1251–1260.e54 (2021).
26. A. Smertenko *et al.*, Plant cytokinesis: Terminology for structures and processes. *Trends Cell Biol.* **27**, 885–894 (2017).
27. E. Lipka, A. Herrmann, S. Mueller, Mechanisms of plant cell division. *Wiley Interdiscip. Rev. Dev. Biol.* **4**, 391–405 (2015).
28. P. Du *et al.*, AtMAC stabilizes the phragmoplast by crosslinking microtubules and actin filaments during cytokinesis. *J. Integr. Plant Biol.* **65**, 1950–1965 (2023).
29. H. Li *et al.*, Arabidopsis MAP65-4 plays a role in phragmoplast microtubule organization and marks the cortical cell division site. *New Phytol.* **215**, 187–201 (2017).
30. P. Dahiya, K. Bürstenbinder, The making of a ring: Assembly and regulation of microtubule-associated proteins during preprophase band formation and division plane set-up. *Curr. Opin. Plant Biol.* **73**, 102366 (2023).
31. A. Smertenko *et al.*, Phragmoplast microtubule dynamics–a game of zones. *J. Cell Sci.* **131**, jcs203331 (2018).
32. M. Abu-Abied *et al.*, Myosin XI-K is involved in root organogenesis, polar auxin transport, and cell division. *J. Exp. Bot.* **69**, 2869–2881 (2018).
33. C. H. Huang, F. L. Peng, Y. J. Lee, B. Liu, The microtubular preprophase band recruits Myosin XI to the cortical division site to guide phragmoplast expansion during plant cytokinesis. *Dev. Cell* **59**, 2333–2346.e6 (2024), 10.1016/j.devcel.2024.05.015.
34. S. Z. Wu, M. Bezanilla, Myosin VIII associates with microtubule ends and together with actin plays a role in guiding plant cell division. *Elife* **3**, e03498 (2014).
35. C. R. Hawes, B. E. Juniper, J. C. Horne, Low and high voltage electron microscopy of mitosis and cytokinesis in maize roots. *Planta* **152**, 397–407 (1981).
36. J. M. Seguí-Simarro, J. R. Austin II, E. A. White, L. A. Staehelin, Electron tomographic analysis of somatic cell plate formation in meristematic cells of Arabidopsis preserved by high-pressure freezing. *Plant Cell* **16**, 836–856 (2004).
37. K. Knox *et al.*, Putting the squeeze on plasmodesmata: A role for reticulons in primary plasmodesmata formation. *Plant Physiol.* **168**, 1563–1572 (2015).
38. Z. P. Li *et al.*, Plant plasmodesmata bridges form through ER-dependent incomplete cytokinesis. *Science* **386**, 538–545 (2024).
39. A. Nebenführ, J. A. Frohlick, L. A. Staehelin, Redistribution of Golgi stacks and other organelles during mitosis and cytokinesis in plant cells. *Plant Physiol.* **124**, 135–151 (2000).
40. X. Cheng, M. Bezanilla, SABRE populates ER domains essential for cell plate maturation and cell expansion influencing cell and tissue patterning. *Elife* **10**, e65166 (2021).
41. D. Zhang, T. C. Bidone, D. Vavylonis, ER-PM contacts define actomyosin kinetics for proper contractile ring assembly. *Curr. Biol.* **26**, 647–653 (2016).
42. T. Higaki, N. Kutsuna, T. Sano, S. Hasezawa, Quantitative analysis of changes in actin microfilament contribution to cell plate development in plant cytokinesis. *BMC Plant Biol.* **8**, 80 (2008).
43. T. D. Pollard, J. A. Cooper, Actin, a central player in cell shape and movement. *Science* **326**, 1208–1212 (2009).
44. M. J. Deeks, P. J. Hussey, Arp2/3 and SCAR: Plants move to the fore. *Nat. Rev. Mol. Cell Biol.* **6**, 954–964 (2005).
45. P. Wang *et al.*, Plant VAP27 proteins: Domain characterization, intracellular localization and role in plant development. *New Phytol.* **210**, 1311–1326 (2016).

46. J. Dyachok *et al.*, Plasma membrane-associated SCAR complex subunits promote cortical F-actin accumulation and normal growth characteristics in Arabidopsis roots. *Mol. Plant* **1**, 990–1006 (2008).
47. C. Li *et al.*, TraB family proteins are components of ER-mitochondrial contact sites and regulate ER-mitochondrial interactions and mitophagy. *Nat. Commun.* **13**, 5658 (2022).
48. P. Wang *et al.*, Keep in contact: Multiple roles of endoplasmic reticulum–membrane contact sites and the organelle interaction network in plants. *New Phytol.* **238**, 482–499 (2023).
49. E. Lee *et al.*, Ionic stress enhances ER-PM connectivity via phosphoinositide-associated SYT1 contact site expansion in Arabidopsis. *Proc. Natl. Acad. Sci. U. S. A.* **116**, 1420–1429 (2019).
50. B. K. Nelson, X. Cai, A. Nebenführ, A multicolored set of in vivo organelle markers for co-localization studies in Arabidopsis and other plants. *Plant J.* **51**, 1126–1136 (2007).
51. M. Takeuchi *et al.*, Single microfilaments mediate the early steps of microtubule bundling during preprophase band formation in onion cotyledon epidermal cells. *Mol. Biol. Cell* **27**, 1809–1820 (2016).
52. C. M. McMichael, S. Y. Bednarek, Cytoskeletal and membrane dynamics during higher plant cytokinesis. *New Phytol.* **197**, 1039–1057 (2013).
53. P. Liu, M. Qi, X. Xue, H. Ren, Dynamics and functions of the actin cytoskeleton during the plant cell cycle. *Chin. Sci. Bull.* **56**, 3504–3510 (2011).
54. A. Lebecq, A. Fangain, A. Boussaroque, M. C. Caillaud, Dynamic apico-basal enrichment of the F-actin during cytokinesis in Arabidopsis cells embedded in their tissues. *Quant. Plant Biol.* **3**, e4 (2022).
55. A. M. Monzon, A. Hatos, M. Necci, D. Piovesan, S. C. E. Tosatto, Exploring protein intrinsic disorder with MobiDB. *Methods Mol. Biol.* **2141**, 127–143 (2020).
56. S. E. Murphy, T. P. Levine, VAP, a versatile access point for the endoplasmic reticulum: Review and analysis of FFAT-like motifs in the VAPome. *Biochim. Biophys. Acta* **1861**, 952–961 (2016).
57. J. A. Slee, T. P. Levine, Systematic prediction of FFAT motifs across eukaryote proteomes identifies nucleolar and eisosome proteins with the predicted capacity to form bridges to the endoplasmic reticulum. *Contact (Thousand Oaks)* **2**, 1–21 (2019).
58. J. Abramson *et al.*, Accurate structure prediction of biomolecular interactions with AlphaFold 3. *Nature* **630**, 493–500 (2024).
59. I. Karahara, L. A. Staehelin, Y. Mineyuki, A role of endocytosis in plant cytokinesis. *Commun. Integr. Biol.* **3**, 36–38 (2010).
60. C. G. Rasmussen, M. Bellinger, An overview of plant division-plane orientation. *New Phytol.* **219**, 505–512 (2018).
61. H. Buschmann, S. Müller, Update on plant cytokinesis: Rule and divide. *Curr. Opin. Plant Biol.* **52**, 97–105 (2019).